

# Effects of Internal Reflections on The Performance of Lens-Integrated mmW and THz Antennas

Burak Ozbey and Kubilay Sertel

ElectroScience Laboratory, Ohio State University, Columbus, OH 43212

Email: ozbey.2@osu.edu, sertel.1@osu.edu

**Abstract**—Multiple reflections from electrically large hemispherical lens surfaces of lens-integrated antennas are investigated using an iterative Huygens’ integral approach. In particular for mmW- and THz-band applications, double-slot antennas on extended hemispherical high-resistivity Silicon lenses have been widely used due to the high Gaussicity of their radiation/reception patterns. Previous studies assumed an electrically-large lens and evaluated the antenna pattern using first-order physical optics approximation. Although this approach is fairly accurate for estimating the radiation pattern of such antennas, the reception pattern and the associated performance of receiving sensors need a more careful consideration due to the relatively large level of internal reflections from the concave boundary of the high index lens. Here, we present an iterative method to compute and study the effects of multiple reflections inside electrically large lenses. The rich nature of quasi-optical wave behavior is demonstrated through several examples corresponding to individual bounces of the incident, reflected, and transmitted waves from a double slot antenna.

## I. INTRODUCTION

Lens-integrated antennas have been very popular for mmW and THz sensor applications due to key advantages that allow efficient coupling to quasi-optical systems. Most importantly, the high Gaussicity and absence of spherical aberrations, coupled with high directivity make such sensors the preferred choice for various sensing and imaging applications [1]–[4]. Although the ideal lens shape is elliptical, hyperhemispherical and extended hemispherical lenses perform equally well in terms of quasi-optical coupling performance. Typically, an electrically large lens is used to collimate slot antenna radiation (typically  $30\lambda$  in diameter), making their computational analysis quite challenging. To address this, a ray-optics/field integration approach was employed by Filipovic et al. in [1] and [2] to find the radiation patterns at the boundary and outside the lens. However, this approach ignores the effect of multiple reflections inside the lens. Although internal reflections in the lens do not significantly impact the radiation pattern of a transmitting antenna, in receiving mode the internal bounces degrade the signal quality and deserve a more accurate analysis. Internally-reflected power can be quite significant, particularly for high dielectric constant materials such as high-resistivity Silicon. In this paper, we study the effects of such multiple reflections within an extended hemispherical lens, integrated with a double-slot antenna. Multiple internal reflections from the lens-air interface, as well as the cylindrical

extension section and the ground plane are taken into account, and their effects on the lens performance are examined.

## II. ANALYSIS OF MULTIPLE INTERNAL REFLECTIONS IN LENS-INTEGRATED ANTENNAS

The geometry of the extended hemispherical lens considered here is shown in Fig. 1. The aperture fields (viz. magnetic currents) of the double-slot antenna with a slot length  $0.28\lambda_{air}$  and a spacing of  $0.16\lambda_{air}$  inside a high-resistivity Silicon ( $\epsilon_r = 11.7$ ) lens are used to calculate the radiation pattern, assuming radiation into the material half space and a first-order Fresnel transmission through the lens-air boundary [1], [2]. For a representative frequency of 246 GHz, an extension length of  $L = 7.3\lambda_d$ , and a  $19\lambda_d$  radius lens result in a physically-compact 13.7 mm diameter lens ( $\lambda_d$  is the wavelength inside the lens). The antenna is located at the center of the  $xy$ -plane, and the slots are along the  $y$ -direction.

The radiated fields inside and outside the lens are shown in Fig. 2, by including the multiple paths shown in Fig. 1. That is, although a sizable portion of the radiated field ( $E_{i,1}$ ) is transmitted through the lens ( $E_{t,1}$ ), a significant amount is also reflected back at the air-lens boundary ( $E_r$ ). This reflected field converges to a “conjugate” focal point inside the Silicon lens and subsequently impinges on the antenna ground plane (i.e. the original focal plane of the extended hemispherical lens), before reflecting back to the lens-air boundary one more time ( $E_{i,2}$ ).  $E_r$  can be calculated by finding the equivalent current densities using the reflected fields on the lens-air boundary, and then radiating them back into the lens using Huygens’ integrals. For evaluating the integrals, Stratton-Chu formulation is preferred since the gradient of Green’s function is defined at the source region and hence it is easier to perform. For completeness, it is given here in the form [5]:

$$\mathbf{E}(\mathbf{r}) = \iint_{S'} \{i\omega\mu[\hat{n} \times \mathbf{H}(\mathbf{r}')]g(\mathbf{r}, \mathbf{r}') + [\hat{n} \cdot \mathbf{E}(\mathbf{r}')]\nabla'g(\mathbf{r}, \mathbf{r}') \\ + [\hat{n} \times \mathbf{E}(\mathbf{r}')] \times \nabla'g(\mathbf{r}, \mathbf{r}')\}dS' \quad (1)$$

We also note that the wave reflected from the ground plane ( $E_{i,2}$ ) can also be computed using image theory. The conventional, first-order transmitted field outside the lens from a radiating double slot antenna is shown in Fig. 2(a), with the inset on the right illustrating instantaneous field distribution inside the extended hemispherical lens. As seen, the first-order

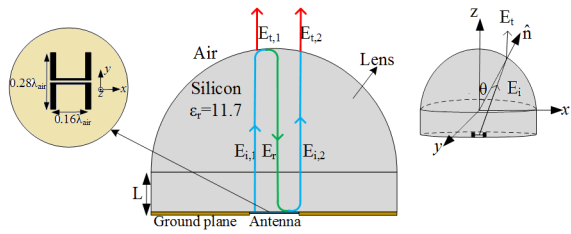


Fig. 1. Geometry of a typical lens-integrated antenna, illustrating the multiple reflection and transmission paths internal to the lens. A 3-d view is shown in the bottom left inset.

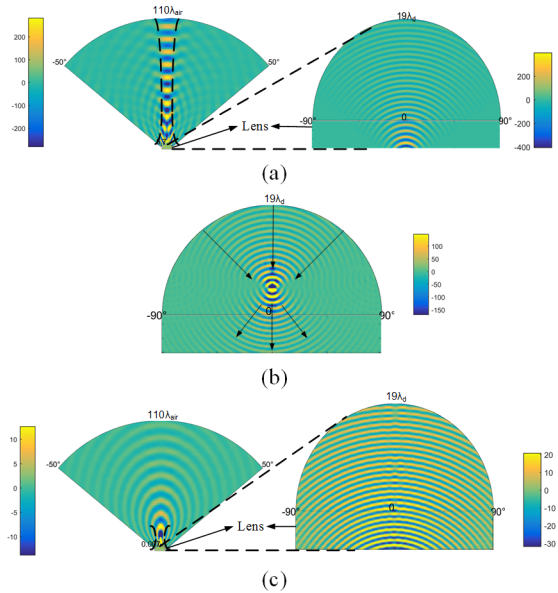


Fig. 2. Incident and transmitted instantaneous fields computed inside and outside the extended hemispherical lens. a)  $E_{t,1}$  and  $E_{i,1}$ :  $x$ -component of the first-order incident (right) and transmitted (left) electric fields on E-plane at a time instant,  $t = 0$ , b)  $E_r$ :  $x$ -component of the first-order reflected electric field on E-plane at a time instant,  $t = 0$ , c)  $E_{i,2}$  and  $E_{t,2}$ :  $x$ -component of the second-order incident electric field (right) and the second-order transmitted (left) electric field on E-plane at a time instant,  $t = 0$ .

transmitted wave has a fairly collimated Gaussian beam profile with its waist occurring at about  $25\lambda_0$  away from the lens surface.

The instantaneous  $E$ -field reflected back into the lens is depicted in Fig. 2(b). As seen, the reflected beam first focuses back to the conjugate focal point of the ellipse that is approximated by the extended hemispherical geometry, before it diverges and reflects from the ground plane on the original focal plane. Fig. 2(c) illustrates the Gaussian beam nature of the second-order transmitted  $E$ -field ( $E_{t,2}$ ). It is interesting to note here that the beam waist and focal point of this second-order field is completely different from the first-order transmitted wave  $E_{t,1}$ , in that the beam waist of  $E_{t,2}$  is much narrower and the focal point for  $E_{t,2}$  occurs very close to the lens surface, at about  $5\lambda_0$  away. The antenna radiation pattern is shown in Fig. 3. As seen, the side lobes are more prominent when the second-order reflection contributions are

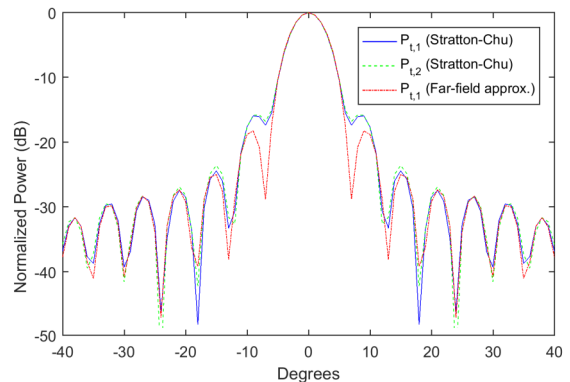


Fig. 3. Computed  $E$ -plane radiation pattern for the first-order transmitted wave (solid) compared to the computed pattern after multiple reflections inside the lens using Stratton-Chu evaluation of equivalent sources on the lens boundary (dashed), and pattern calculated using far-field approximation (dash-dotted).

included in the calculation. Furthermore, it is observed that the Stratton-Chu formulation yields a much shallower first null, as well as a higher side lobe level, as compared to the far-field approximation used in [1], [2]. Finally, the far-field patterns obtained from Stratton-Chu formulation agrees better with the experiment results given in [1].

### III. CONCLUSION

In this paper, the effects of multiple reflections within a lens-integrated double-slot antenna are investigated. The fields incident on the lens-air boundary are evaluated using the radiation pattern of a double-slot antenna on a dielectric interface. Subsequently, utilizing Huygens' principle, the fields reflected from the boundary are calculated by employing the equivalent current densities within the Stratton-Chu framework. Image theory is also utilized to find the fields that reflect back from the ground plane, which are subsequently transmitted through the lens boundary as a second-order radiation effect. It is shown that the contributions from multiple reflections yield higher side-lobe levels, and should be considered for a more accurate characterization of lens-integrated antenna structures.

### ACKNOWLEDGMENT

The authors would like to thank the Turkish Fulbright Commission for their support under the Postdoctoral Program Grant.

### REFERENCES

- [1] D. F. Filipovic et al., "Double slot antennas on extended hemispherical and elliptical silicon dielectric lenses," *IEEE Trans. Microw. Theory Techn.*, vol. 41, no. 10, pp. 1738–1749, Oct. 1993.
- [2] D. F. Filipovic et al., "Off-axis properties of silicon and quartz dielectric lens antennas," *IEEE Trans. Microw. Theory Techn.*, vol. 45, no. 5, pp. 760–766, May 1997.
- [3] G. C. Trichopoulos et al., "A novel approach for improving off-axis pixel performance of terahertz focal plane arrays," *IEEE Trans. Microw. Theory Techn.*, vol. 58, no. 7, pp. 2014–2021, Jul. 2010.
- [4] G. C. Trichopoulos et al., "A broadband focal plane array camera for real-time THz imaging applications," *IEEE Trans. Antennas Propag.*, vol. 61, no. 4, pp. 1733–1740, Apr. 2013.
- [5] J. A. Kong, *Electromagnetic Wave Theory*, John Wiley & Sons, 1986.